Vulnerability in Public Transportation Networks

Aaron Aquino[1], Noah Gamboa[2], and Antariksh Mahajan[3]

[1]*aquino@stanford.edu*
[2]*ngamboa@stanford.edu*
[3]*am95@stanford.edu*

I. Introduction

Transportation networks are indispensable to the lives of people in cities. In Europe, metros alone carry 31.6 million passengers a day [12]. However, this means that the impact of disruptions in transport networks can have particularly severe consequences. Following the 2005 London bombings, which simultaneously targeted several stations in the London Underground, subway passenger ridership was down 30% on weekends and 15% on weekdays even months later [3]. Given both the importance and the fragility of public transit networks (PTNs), PTN vulnerability has become an important area of research for city planning. In particular, using network analysis techniques to analyze PTN vulnerability can shed light on where new routes and stations can be added to an existing system to enhance its resilience in the face of disruptions such as failing infrastructure, severe weather, or targeted attacks.

This project examines the PTN in Madrid, Spain. Madrid was the city of choice for several reasons. It is heavily utilized, and thus important to many people: in 2013, almost 1.37 billion trips were taken on the PTN [4]. It is also interesting to study because it is complex, with five individual transit types comprised of two metro, two bus, and a train system. Vulnerability analysis on Madrid's PTN is particularly relevant given the 11-M train bombings in 2004, which killed more than 190 people [14]. Finally, data on this PTN is available for all five transit types in a standardized format.

By analyzing an aggregate PTN graph that links all five public transportation types, we aim to test the following hypotheses:

- Edges in the city center are the most critical. The precise definition of criticality will be explored in detail in Section IV, but at a high level, a critical edge is one whose disruption would cause the most harm to the system.
- When going from a network containing one transport type to many, network diameter will increase, but average travel time between stations will decrease. For example, a network containing only the bus system will have a smaller diameter but longer average travel time between any two stations than a network containing all five transport types.
- Nodes with the smallest weighted clustering coefficients occur at the geographical extremes of the network. A rigorous, mathematical definition of weighted clustering coefficient is given in Section IV, but at a high level, this means that people who take public transport from the geographical extremes of the network tend to have fewer options for where they start their journeys.

Based on our investigation of these hypotheses, we aim to propose improvements to Madrid's PTN through the addition of new stops and routes.

II. Literature Review

Vulnerability has two key components: the probability of disruption and the consequences of disruption [6]. To illustrate the difference between the two, a station could have high probability of disruption if its infrastructure were aging, but limited consequences if it were used by very few people. Jenelius et al. chose to define vulnerability based solely on the consequences of disruption, since probability was difficult to measure using network properties. They then used the following definition of vulnerability: "a node is vulnerable if loss (or substantial degradation) of a small number of links significantly diminishes the accessibility of the node, as measured by a standard index of accessibility". They applied this definition to vulnerability in road networks, where their standard of accessibility was the cost of travel, which increased when parts of the road network were disrupted. They also identified two perspectives on this measure of cost: "equal opportunity", where all network edges were considered equal, and "social efficiency", where edges were weighted by how many people traveled on them per unit time.

Other studies used similar definitions of vulnerability, but different accessibility indices. Rodríguez-Núñez and García-Palomares used the index of time instead of cost to analyze the metro network in Madrid [9]. In other words, they measured the vulnerability of a station by analyzing the expected increase in average travel time from that station to any other station when a random network link was disrupted. They used the "social efficiency" framework as defined by Jenelius et al., where the travel time between any two stations was weighted by how frequently people made the trip between those two stations. They also defined the term "criticality" for an edge (as opposed to vulnerability, which is defined for a node) as the average increase in travel times across the network when that edge is disrupted. Identical definitions were used by Taylor in a study on vulnerability and traffic incidents, showing that these are metrics used consistently in the literature [11].

Even with a given definition of vulnerability, there are different ways of modeling PTNs using graphs. Sienkiewicz and Holyst identify two possible topologies [10]. The first is $\mathbb{L}$-space, which is more representative of PTNs in their real, physical form: nodes represent stops and edges represent transitions between consecutive stops. The other is $\mathbb{P}$-space, where nodes represent stops but edges exist between stops that can be reached from each other without transfers. In other words, if a particular bus or train travels along a set of stops S on a particular route, then the stops in S form a complete subgraph of the broader network. These two topologies show different types of relationships in the PTN; $\mathbb{L}$-space models patterns in stops, whereas $\mathbb{P}$-space models patterns in routes. Von Ferber et al. identify other topologies such as $\mathbb{B}$-space (bipartite graph where both routes and stations are nodes) and $\mathbb{C}$-space (only routes are nodes), but stated that they provided less insight than $\mathbb{L}$- and $\mathbb{P}$-spaces, hence they are not within the scope of this paper [13].

Once a network topology is chosen, various properties of the network can be calculated. Latora and Marchiori introduced the concept of network efficiency, a measure of how fast information flows across a network [7]. When analyzing the efficiency of the Boston PTN, they found that efficiency changed significantly when looking purely at the subway versus looking at both bus and subway, which provides a strong motivation for our project to account for all types of transit. Von Ferber et al. chose to calculate several properties of PTNs for fourteen different cities, including average node degree, maximal and mean shortest path length, betweenness centrality, and the ratio of mean clustering coefficient to random graphs of the same size [13]. They then used these properties to identify interesting statistical patterns, such as the diversity in degree distributions of PTNs in different cities. However, they did not use these findings to draw insights on how these PTNs could be improved, which motivated our approach of posing hypotheses and testing them against the actual network.

Finally, these properties can be recalculated based on various scenarios to analyze the network's resilience. Murray et al. identified three increasingly broad approaches to scenario-based calculations: scenario-specific, which only accounts for particular disruptions; strategy-specific, which accounts for multiple disruptions based on a strategic attacker; and simulation, which creates random scenarios [8]. The choice of approach depends on one's objectives as well as computational resources. This project focuses on the strategy-specific approach, since this can help city planners to deal with worst-case scenarios where the most important links in the network are disrupted.

III. Model

Data from Madrid's governing transport body, the Consorcio Regional de Transportes de Madrid (CRTM), was used to construct our graphs. The data was published in General Transit Feed Specification (GTFS) format, a standardized format for specifying PTNs that includes data such as stop locations, fares, routes, and time taken between stops. A full specification of GTFS can be found in [1].

GTFS data from September 2017 was used from five different transit types: Metro (subway), EMT (bus), Metro Ligero (subway), Autobuses Urbanos (bus), and Cercanías (train). A node was created for every stop in every network. A visualization of the physical locations of Metro, EMT, and Autobuses Urbanos nodes is shown in Figure 1. The value of connecting different networks can immediately be seen: many locations have stops for different types of public transport located close to each other, showing that there are multiple ways of getting between destinations. Moreover, different networks have different densities of stops inside and outside the heart of the city. For example, the blue nodes (EMT) are highly dense within the heart of the city, while the yellow nodes (Autobuses Urbanos) have clusters outside the city center.

Subsequently, edges were created using both the $\mathbb{P}$- and $\mathbb{L}$-space topologies (see Section II). This created five different disjoint subgraphs, one for each type of transit.

Fig. 1: Physical locations of metro (red), EMT (blue), and Autobuses Urbanos (yellow) stops. Other networks are excluded for simplicity.

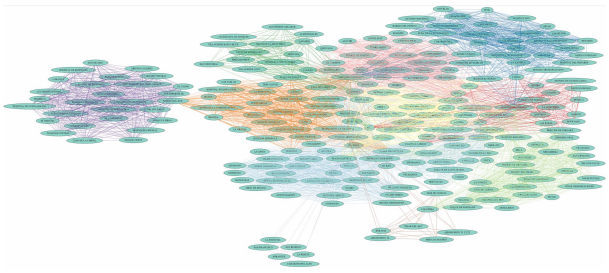

Fig. 2: Metro subgraph. Each color represents a metro line.

Figure 2 shows the subgraph for the metro system, with different colors representing different metro lines.

Finally, in both the $\mathbb{P}$- and $\mathbb{L}$-space, edges were added between stops that were within 100m of each other, both across subgraphs and within subgraphs. The distances were calculated using the standard WGS-84 ellipsoid conversion from latitude-longitude coordinates to distance across the surface of the earth. It is important to note that these added edges were conceptually different in the two spaces. In the $\mathbb{L}$-space, traversing an added edge represented walking between closely-located stops as traveling another "stop". On the other hand, in the $\mathbb{P}$-space, traversing an added edge represented walking between closely-located stops as a transfer between forms of transport. Figure 3 shows visualizations for both spaces, where it can be seen that the $\mathbb{P}$-space is far more dense, since stops on any given route form a complete subgraph instead of a chain. In total, the $\mathbb{L}$-space graph had 6,587 nodes and 20,540 edges, whereas the $\mathbb{P}$-space graph had 6,587 nodes and 590,976 edges.

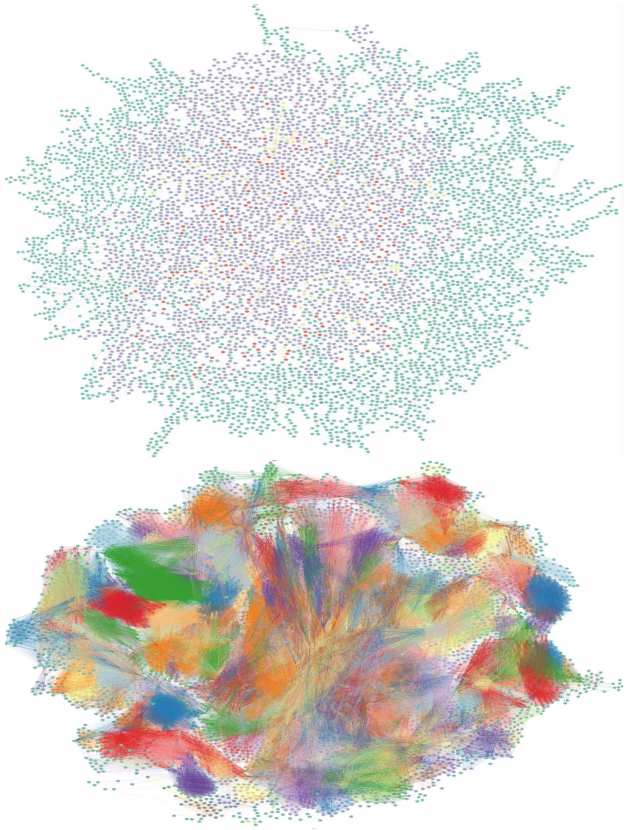

Fig. 3: $\mathbb{L}$- (above) and $\mathbb{P}$- (below) space graphs of the full network. It is clear that the $\mathbb{P}$-space graph is more dense, since stops along common routes form complete subgraphs.

IV. Important Equations

This section details important equations for calculating criticality, which is crucial for evaluating our first hypothesis. Along the way, we will detail how to calculate average travel times, which are important for evaluating our first hypothesis.

First, we use travel times as our metric of accessibility. Given the shortest possible travel time between any two stations (found using Dijkstra's algorithm as described in Section V), we can calculate the average travel time from a station i to every other station. We use the "equal opportunity" approach to accessibility, meaning that every trip is treated as equal, so the average travel time from station i is:

$$\bar{T}_i = \frac{1}{n-1} \sum_j T_{ij},$$

where T_{ij} is the travel time from station i to station j and n is the total number of nodes in the network. Given

T_i for all $1 \leq i \leq n$, we can calculate the overall average travel time in the network:

$$\bar{T_0} = \frac{1}{n} \sum_i \bar{T_i}$$

Next, we analyze the impact of disruption of each individual link. However, it is necessary to note that disrupting a link can result in the graph becoming disconnected, thus making travel times between certain nodes infinite. Thus we have to account for the nodes which become disconnected, and the nodes for which the travel times simply increase (or stay the same). For the latter case, let the set of stations which are still reachable from station i once edge a is disrupted be $A_{i,a}$. Then the new average travel time from station i is given by:

$$\bar{T}_{i,a} = \frac{1}{|A_{i,a}|} \sum_{j \in A_{i,a}} T_{ij}$$

The unsatisfied demand, or number of nodes that become disconnected from station i when edge a is disrupted, is:

$$d_{i,a} = |V \setminus A_{i,a}|$$

And the new overall average travel time in the network is:

$$\bar{T_a} = \frac{1}{n} \sum_i \bar{T}_{i,a}$$

It is important to note that, since our network used many different transportation types, there were no cases where removing an edge disconnected the graph. However, the above equation on unsatisfied demand is still included for completeness.

We then measure the criticality of each link a by the change in overall travel time when that link is disrupted:

$$C_a = \bar{T_a} - \bar{T_0}$$

A final important equation is related to clustering coefficients. Since we are using weighted edges, we use a proposed generalization of the clustering coefficient formula to weighted graphs [2]:

$$c_i = \frac{1}{s_i(k_i - 1)} \sum_{j,h} \frac{w_{ij} + w_{ih}}{2} a_{ij} a_{ih} a_{jh}$$

s_i is the sum of the weights of node i's outgoing edges and k_i is the degree of node i, while a denotes entries in the adjacency matrix.

V. Algorithms

A. Paths with shortest travel times

In order to compute the shortest trips between all pairs of nodes in our aggregate network, we implemented a version of Dijkstra's algorithm that takes a single source node and then calculates the shortest paths from the source to every other node in the network. At a high level, Dijkstra's initially assigns a tentative distance value of infinity to every destination node. It then iterates over all previously unvisited nodes and for each one, computes a new tentative distance to that node based off its neighbors. If this new tentative distance is less than the previous one, then the value is updated. When the algorithm finishes, each node now stores the length of the shortest path from the source to that node. Our version of Dijkstra's also records the specific nodes in each shortest path by keeping track of each destination's previous node.

The original implementation of Dijkstra's runs in $O(|V^2|)$ time, but we decided to implement a variation created by Fredman and Tarjan that utilizes a Fibonacci heap and has a runtime of $O(|E| + |V| \log |V|)$ [15]. This gain in efficiency comes from three special heap operations, `add_with_priority()`, `decrease_priority()` and `extract_min()`, which allow the algorithm to process nodes in order of increasing tentative distance.

To speed up our computations, we used multithreading when running Dijkstra's over all the nodes in our network. For a given node, we then calculated the average over each of its shortest paths to determine the farness centrality, or mean travel time from that node.

B. Criticality

Given the size and density of the graphs, calculating the overall criticality was computationally infeasible. Even with multithreading, it took about an hour to calculate the criticality of an edge, which means it would have many months of non-stop computation to calculate the criticality of every edge.

To bring the criticality calculations to within our computational limits, we chose to sample a subset of the edges to calculate their criticality. In order to gain an understanding of criticality inside and outside the city center, edges were sampled separately from within and outside the city center. We defined the city center as all points within 5km of Puerta del Sol, which was the central address of Madrid as defined by the Google Maps Reverse Geocoding API [5].

Station name	Transit type	Average travel time (s)
Sol	Cercanías	1838
Tribunal	EMT	1854
Alonso Martínez	EMT	1855
Gran Vía	Metro	1859
Callao	EMT	1870

Fig. 4: Lowest 5 average travel times in the aggregate graph.

To calculate criticality, the average travel time $\bar{T}_i$ from each node in the original graph were initially stored. During the running of Dijkstra's algorithm to calculate these values, a map of each edge to a list of source-destination node pairs whose shortest path passed through that edge was also computed and stored. Next, for each edge sampled from the graph, the edge was deleted, and Dijkstra's algorithm was reapplied to all the source-destinations pairs whose old shortest paths passed through that edge. The old average travel times were updated, and the new $\bar{T}_{i,a}$ was calculated for each node. Using the updated average travel times for each node, the criticality of the removed edge was found.

VI. Results

A. Hypothesis 1: Edges in the city center are the most critical.

Our analysis of criticality began with travel times as our metric of accessibility. The GTFS feeds specified travel times for each stop on each route, and those travel times were added to the graph as edge weights. In addition, a flat 3-minute weight was added to each edge that was added for stops within 100m of each other.

As described in Section V, average travel times are calculated based on the shortest possible travel time between any two stations. To find this path from each node to every other, we ran Dijkstra's algorithm for each node as described in Section VI. We found the five stations with the shortest average travel time $\bar{T}_i$, shown in Figure 4. As a quick sanity check, Sol is the station in one of the busiest and most well-known public squares in Madrid, so it is unsurprising that this station is the most central (where centrality is measured by average travel time).

Station name	Transit type	Average travel time (s)
Av. Berlín-Florencia	Autobuses Urbanos	92610
Bronce-Platino	Autobuses Urbanos	89865
Concejal V.Granizo-Victoria Kent	Autobuses Urbanos	87886
Av .Concordia-Marqués de Hinojosa	Autobuses Urbanos	87666
Av. Juan Gris-Pirineos	Autobuses Urbanos	87367

Fig. 5: Highest 5 average travel times in the aggregate graph.

Conversely, we found the five stations with the longest average travel time $\bar{T}_i$, shown in Figure 5. Another quick sanity check tells us that Av. Berlín-Florencia is on the distant eastern outskirts of Madrid, which explains its long average travel time.

Figure 6 shows a plot of criticality vs. distance of the source node from the city center for a few edges. Only a small sample of edges was included so as to make this plot less noisy. It is clear that there is no obvious pattern in the plot; there are small criticality values scattered throughout, while the peaks are inconsistent. However, we can see that the highest criticality values tend not to occur very near the city center or very far from it, but at the intermediate distances. This could suggest that the city center is already sufficiently resilient to disruption or attack, since it already has many alternative routes within it. Thus, the truly critical edges have become those between the city center and the surrounding districts, which are interfaces between residential areas and the city center that are less well-served by public transportation. This implies that it might serve policymakers well to focus more on creating alternative routes for intermediate-distance stops, since they could cause severe delays in the case of disruption.

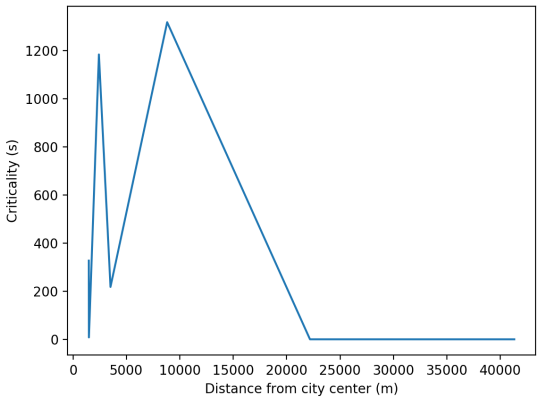

Fig. 6: Criticality of node vs. distance from city center (m).

Network	$\mathbb{L}$-graph Diameter	$\mathbb{P}$-graph Diameter
Full Network	78	9
Autobuses Urbanos	92	11
Cercanías	14	3
EMT	55	5
Metro	44	4
Metro Ligero	27	2

Fig. 7: Graph diameters for the aggregate network and each subnetwork.

B. Hypothesis 2: When going from a network containing one transport type to many, network diameter will increase, but average travel time between stations will decrease.

We define diameter as the longest shortest path over the network. We looked at each of the individual networks and the aggregate of all 5 networks and evaluated the diameter for each, and the results are shown in Figure 7. Our hypothesis is that the diameter of the full network would be longer than the diameter of the individual networks. The results confirm this hypothesis for some networks, but not others. Overall, we see an averaging effect amongst the different networks, where the diameter of the aggregate network is somewhere between the diameters of the original subnetworks.

We can understand this phenomenon by looking at the original diameter for the Autobuses Urbanos (AU) network. Figure 7 shows that AU is by far the largest subnetwork of the 5 with nearly an order of magnitude

Network	$\mathbb{L}$-graph Mean Path Length	$\mathbb{P}$-graph Mean Path Length
Full Network	11.13	2.57
Autobuses Urbanos	17.70	3.066
Cercanías	4.97	1.75
EMT	20.13	2.72
Metro	14.55	2.16
Metro Ligero	17.73	3.65

Fig. 8: Average path lengths for the aggregate network and each subnetwork.

larger diameter than the rest of the subnetwork. This means that adding it to the other networks will increase the overall network diameter. To illustrate this phenomenon, consider the addition of the AU network (large diameter) to the Cercanías network (small diameter). The original AU network has many bus stops that are not very densely connected, hence its large original diameter. When combined with other Cercanías stops that allow shortcuts between bus stops, the aggregate diameter decreases, but there are still many bus stops that require many steps to reach. Conversely, from the point of view of the Cercanías network, adding the AU stops increases the number of stops that can be reached without proportionately increasing the number of edges between them, thus the network diameter increases. Overall, when combined with the other networks, the longest shortest path shrinks by 15% and 18% for $\mathbb{P}$- and $\mathbb{L}$-space graphs respectively, as compared to the AU network.

Another observation is that the $\mathbb{P}$-graph diameters are all significantly smaller than their $\mathbb{L}$-space counterparts. However, since we know that the former is far more densely connected, this is an unsurprising result.

We now turn to average travel time. The results for the calculations for the aggregate graph, as well as each subnetwork, are shown in Figure 8.

The first essential observation from Figure 8 is that, in the $\mathbb{L}$-space graph, the average travel time for the aggregate graph is far smaller than that of almost all the other networks (with the exception of Cercanías). This lends support to the motivation behind our project, since it illustrates how combining different forms of transportation has a significant impact on travel time, and thus a combined network is more likely to be representative of the real world.

Another example of the positive effects of combining

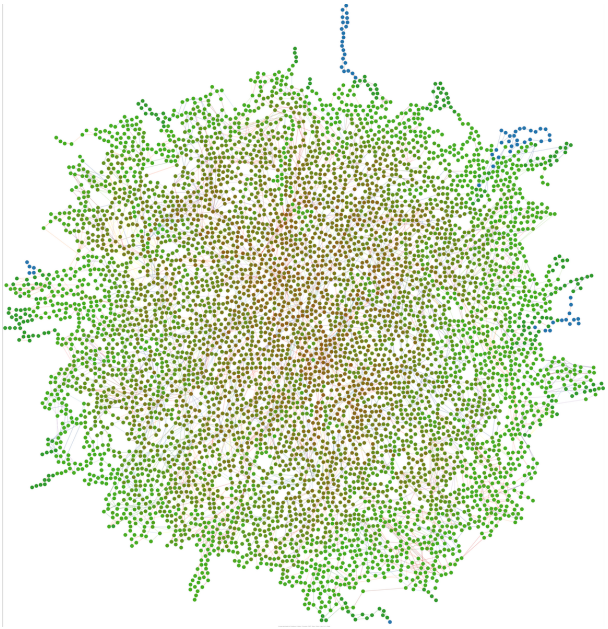

Fig. 9: Heatmap of $\mathbb{L}$-space graph for aggregate network, where nodes with shorter average path lengths are more red.

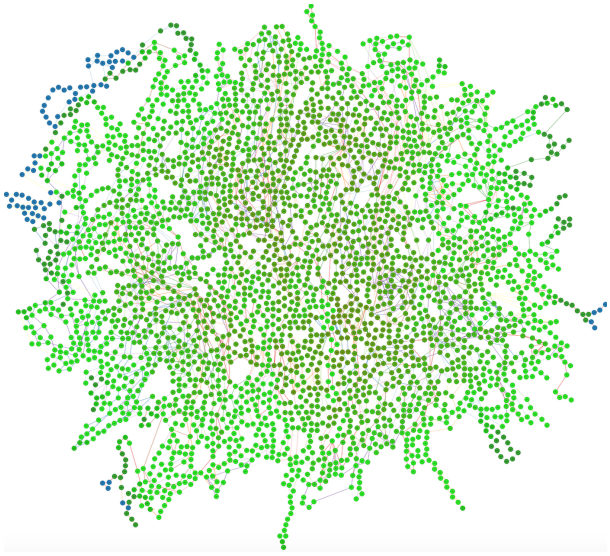

Fig. 10: Heatmap of $\mathbb{L}$-space graph for Autobuses Urbanos, where nodes with shorter average path lengths are more red.

different transit networks can be seen when viewing the graph as a heat map for which the hotter a node gets, the smaller its average path length becomes. To see this, simply compare the aggregate graph (Figure 9) with that for Autobuses Urbanos (Figure 10): it is clear that the former contains more nodes with shorter average path lengths.

Another interesting observation is the relative changes for each graph from the $\mathbb{L}$- to the $\mathbb{P}$-space. For example, we see that out of all the subnetworks, EMT has the greatest reduction in mean path length from $\mathbb{L}$ to $\mathbb{P}$. This suggests that it has many long lines with few transfers. Meanwhile, in both spaces, the aggregate network has a smaller mean path length than the EMT subnetwork. One question that this raises is: how do groups of subnetworks interact with each other? For instance, how much does the mean path length for the EMT graph decrease when paired with each other network? This can shed light on interactions between subnetworks, and possibly give transportation planners some insight into the synergies between different transportation types.

C. Hypothesis 3: Nodes with the smallest clustering coefficients occur at the geographical extremes of the network.

The original justification for this hypothesis was that interchanges and intersections tend to occur close to each other more in the city center than anywhere else, thus clustering coefficients should be higher in the city center. However, the results suggest that the answer may be more nuanced.

Figure 11 shows the geographic distribution of weighted clustering coefficients (see Section IV) for the $\mathbb{L}$-space graph, where darker colors represent higher clustering coefficients. It is evident that the darkest colors are not clustered in the city center; rather they are spread out throughout the city, including in its outskirts. Note that in this case, the weights are travel times; therefore, darker colors represent node clusters where it takes a long time to get between nodes in that cluster.

The existence of dark-colored nodes in the outskirts is unsurprising. Suburbs are likely to have fewer and less frequent public transport connections, so traveling times are likely to be higher. However, the darker spots closer to the city center are more surprising. These suggest that, in spite of being close to the city center, there are certain pockets of nodes that are not very well-connected in terms of short traveling times. This may reveal pockets of public transport nodes that the government should look to improve.

Next, Figure 12 shows a similar visualization for the $\mathbb{P}$-space graph. Here, the results are less surprising. We see dark colors throughout the city including on the outskirts, showing that there long transfer times throughout the city. However, we also see a collection of lighter points near the city center, showing that transfer times

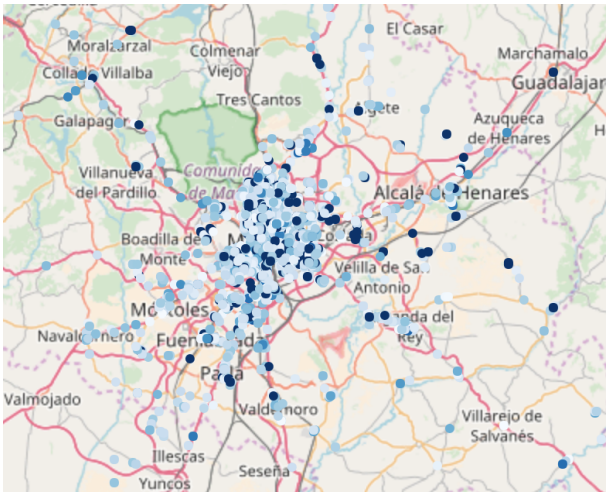

Fig. 11: Weighted clustering coefficients for $\mathbb{L}$-space graph. Note that nodes with clustering coefficients of 0 are excluded for clarity.

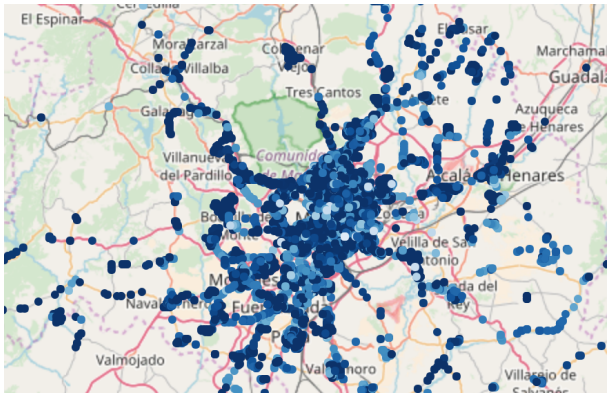

Fig. 12: Weighted clustering coefficients for $\mathbb{P}$-space graph. Note that nodes with clustering coefficients of 0 are excluded for clarity.

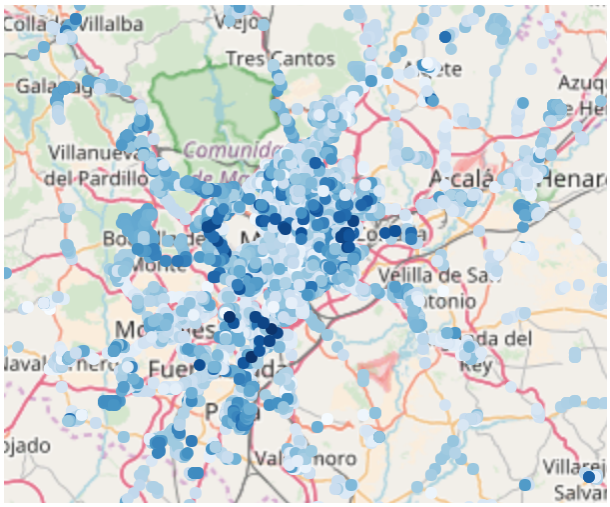

Fig. 13: Unweighted clustering coefficients for $\mathbb{P}$-space graph. Note that nodes with clustering coefficients of 0 are excluded for clarity.

near the city center are shorter due to the better availability of public transport. It is important to observe that this visualization compresses information about many thousands of nodes; a more detailed inspection of this map could reveal more shades of differentiation between more and less well-connected areas in terms of transfer time.

Finally, Figure 13 is the only one that generally confirms our hypothesis. This map shows unweighted clustering coefficients for the $\mathbb{P}$-space, and the higher occurrence of dark spots near the center show that there is a higher availability of transfers near the city center, which is an expected result. However, we can also note that there are pockets with slightly higher clustering coefficients even on the outskirts of the city (e.g., in the southwest). This suggests the existence of suburban centers, where transportation to the suburbs may congregate into hubs. This is an important observation for policy planning: if expanding public transportation to the suburbs, transport planners may want to connect their new lines to these hubs, or to note that the areas around the hubs are already well-served.

VII. Summary and Conclusions

This project aimed to propose improvements to Madrid's PTN through the testing of the three hypotheses proposed in Section I. From hypothesis 1, we were able to identify critical edges that, when removed, significantly impacted the performance of the PTN. Policymakers could consider adding in more parallel transportation methods between the endpoints of those edges to increase resilience to attack. From hypothesis 2, we found that different subnetworks behave differently in the $\mathbb{L}$- and $\mathbb{P}$- spaces, which reveals characteristics about the number of stops versus transfers in those subnetworks. We also learned that exploring different combinations of subnetworks could reveal interesting synergies between transportation types. Finally, hypothesis 3 showed that clustering coefficients can reveal pockets of PTNs that have long travel times between them, and thus can be improved through more frequent public transport service.

VIII. Challenges and Future Work

Future work in this domain would do well to note that the C++ version of the SNAP library has several bugs. In particular, there were several

instances in the `GetWeightedShortestPath()` function where the syntax for retrieving values from HashMaps was incorrect, resulting in hours of frustrating and time-consuming debugging. However, the C++ version does run significantly faster than the Python one, and additionally contains certain functions, such as `GetWeightedFarnessCentr()`, that the latter does not.

Another key challenge faced was lack of descriptive methodology in the literature on creating PTN graphs. For instance, despite the fact that von Ferber et al. analyzed combinations of different transport types [13], they did not describe how edges were created across networks. Future work can continue experimenting with our 100m threshold for creating inter-network edges and 3min weight for these edges to determine how these values affect these results, since we lacked the time and computational power to do so. In addition, while a few papers separately calculated change in average travel time and unsatisfied demand as we did in Section IV, none came up with a holistic measure to combine those two metrics such that the impact of disrupting a link could be measured on a single scale. While this did not impact our project due to the dense connectedness of our networks, it may have an impact on more sparse PTNs.

We also faced difficulties in working with the data itself. We continually uncovered subtleties and new details as we worked with the data; for instance, we found that the GTFS specification had multiple stop IDs for identical stops, which led to duplicate nodes in our graph early on. It is also difficult to check the correctness of our graphs, given their huge size and complexity. However, cross-checking small random samples of the graph with the true PTN network maps was effective in helping us ensure the correctness of our networks.

Finally, computational power was a key resource constraint. In order to calculate the criticality of each edge, we had to recalculate all the shortest paths in the graph and all the average travel times. This meant that it was only possible to calculate a small number of criticality values. Unfortunately, we did not anticipate this constraint, and thus could not gain access to better computational resources in time. Any work that seeks to build on this project should make sure to secure computational resources that can feasibly calculate the values we could not.

One important area for future research is the investigation of different combinations of subnetworks. As mentioned in Section VI, looking at how the one network behaves when paired with various other networks could shed light on pairwise interactions between subnetworks. This could help policymakers improve PTNs across subnetworks; for instance, if they find that AU and Metro complement each other, they could reinforce that synergy through greater AU stop availability near Metro stops.

Overall, this work demonstrates that graphical techniques can be a useful tool in analyzing PTN performance and resilience. Moreover, looking at PTNs in aggregate can yield significantly more practical insights than examining individual subnetworks. While computational power is a power when looking at graphs of such complexity, such analysis has the potential to be a powerful tool in informing policymakers' decisions on how to develop PTNs.

VIII. References

[1] Google Transit APIs. General Transit Feed Specification Reference, October 2017.

[2] A. Barrat, M. Barthelemy, R. Pastor-Satorras, and A. Vespignani. The architecture of complex weighted networks. *Proc Natl Acad Sci U S A*, 101(11):3747–3752, March 2004.

[3] A. Chen, C. Yang, S. Kongsomsaksakul, and M. Lee. Network-based Accessibility Measures for Vulnerability Analysis of Degradable Transportation Networks. *Network Spatial Economics*, December 2007.

[4] Consorcio Regional de Transportes de Madrid. Demanda de transporte pblico colectivo. Technical report, 2013.

[5] Google. Reverse geocoding, 2017. [Online; accessed 6-December-2017].

[6] E. Jenelius, T. Peterson, and L.G. Mattsson. Importance and exposure in road network vulnerability analysis. *Transportation Research Part A: Policy and Practice*, August 2006.

[7] V. Latora and M. Marchiori. Efficient Behavior of Small-World Networks. *Physical Review Letters*, November 2001.

[8] Alan T. Murray, Timothy C. Matisziw, and Tony H. Grubesic. A Methodological Overview of Network Vulnerability Analysis. *Growth and Change*, 39(4):573–592, December 2008.

[9] E. Rodrguez-Nez and J.C. Garca-Palomares. Measuring the vulnerability of public transport networks. *Journal of Transport Geography*, 35:50–63, February 2014.

[10] J. Sienkiewicz and J. A. Hołyst. Statistical analysis of 22 public transport networks in Poland. *Physical Review E*, 72(4):046127, October 2005.

[11] M.A.P. Taylor. Critical Transport Infrastructure in Urban Areas: Impacts of Traffic Incidents Assessed Using Accessibility-Based Network Vulnerability Analysis. *Growth and Change*, November 2008.

[12] Union Internationale des Transports Publics. World Metro Figures. Technical report, October 2010.

[13] C. von Ferber, T. Holovatch, Yu. Holovatch, and V. Palchykov. Public transport networks: empirical analysis and modeling. *The European Physical Journal B*, 68:261–275, 2009.

[14] Wikipedia. 2004 madrid train bombings — Wikipedia, the free encyclopedia, 2017. [Online; accessed 15-November-2017].

[15] Wikipedia. Dijkstra's algorithm — Wikipedia, the free encyclopedia, 2017. [Online; accessed 14-November-2017].